Supporting Information

Pt(II) complexes with a novel pincer N^C^N ligand: synthesis, characterization, and photophysics

Evgeniia E. Luneva[1], Daria O. Kozina[1], Anna V. Mozzhukhina[1], Vitaly V. Porsev[1], Anastasia I. Solomatina[1,*], and Sergey P. Tunik[1,*]

[1] Institute of Chemistry, St. Petersburg State University, Universitetskii av., 26, 198504 St. Petersburg, Russia; yevgeniyalunyova@gmail.com (E.E.L.); kozina.d@yandex.ru (D.O.K.); st101545@student.spbu.ru (A.V.M); v.porsev@spbu.ru (V.V.P.)

* Correspondence: a.solomatina@spbu.ru (A.I.S.); sergey.tunik@spbu.ru (S.P.T)

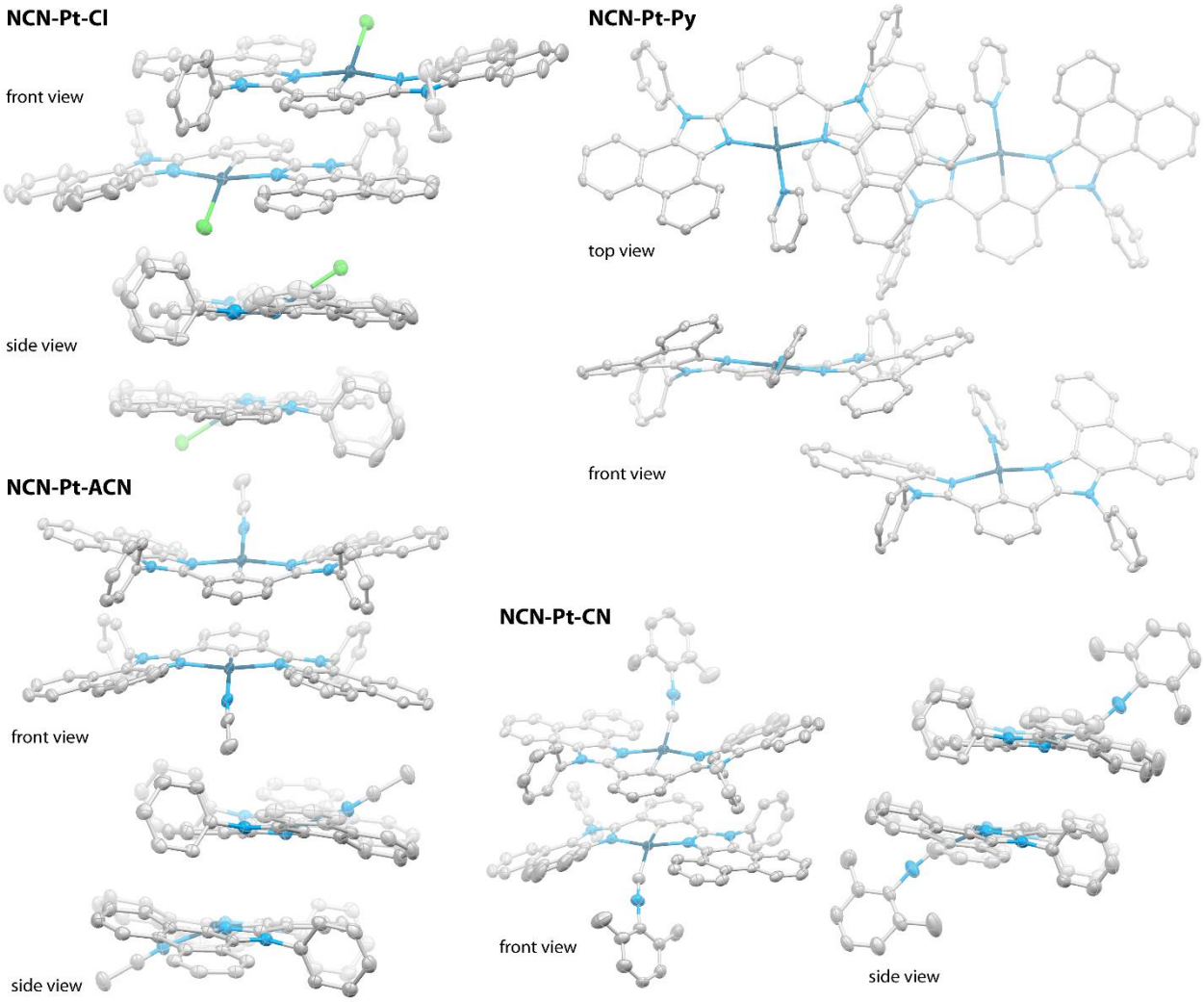

Figure S1. Packing of platinum complexes in solid state showing thermal ellipsoids at the 50% probability level. Hydrogen atoms and counterions are omitted for clarity.

Table S1. Selected bond distances (Å) and angles (°).

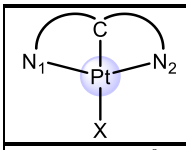	**NCN-Pt-Cl**	**NCN-Pt-ACN**	**NCN-Pt-Py**	**NCN-Pt-CN**	**Pt-Pt**	**Pt-Ag-Pt**
Distances, Å						
Pt-N1	2.056(10)	2.063(4)	2.066(2)	2.048(3)	2.079(5)/ 2.067(4)	2.056(10)/ 2.083(8)
Pt-N2	2.082(9)	2.064(4)	2.071(3)	2.050(3)	2.042(5)/ 2.115(5)	
Pt-C	1.938(11)	1.934(4)	1.961(3)	1.978(3)	1.935(6)/ 1.942(6)	2.058(11)/ 2.050(9),
Pt-X	2.419(3)	2.105(4)	2.127(2)	2.031(4)	2.186(4)/ 2.134(4)	
Pt-Pt					3.1396(3)	
Pt-Ag						2.9762(9)/ 2.9626(9), 2.9643(9)/ 2.9926(9)
Angles, °						
C-Pt-X	156.1(3)	163.53(17)	177.55(12)	160.32(17)	167.9(2)/ 176.0(2)	
N1-Pt-C	80.9(4)	81.09(16)	79.80(12)	79.61(14)	80.1(2)/ 80.0(2)	
N2-Pt-C	80.0(4)	78.89(16)	79.35(12)	79.52(13)	80.5(2)/ 80.4(2)	
N1-Pt-X	98.0(3)	100.29(14)	98.05(10)	99.16(14)	106.31(17)/ 96.27(17)	
N2-Pt-X	101.6(2)	99.74(14)	102.77(10)	101.43(14)	94.86(17)/ 103.44(18)	
N1-Pt-N2	160.2(3)	159.76(15)	159.11(10)	158.94(12)	157.61(19)/ 159.64(19)	
C-Pt1-Pt2					95.08(16)	
Pt1-Pt2-C′					102.97(16)	

Table S2. Crystallographic data for platinum complexes.

Compound	**NCN-Pt-Cl**	**NCN-Pt-ACN**	**NCN-Pt-Py**	**NCN-Pt-CN**	**Pt-Pt**	**Pt-Ag-Pt**
Formula	$C_{48}H_{29}ClN_4Pt$	$C_{56}H_{42.74}F_6N_6OPPt$	$C_{55}H_{38}Cl_4F_6N_5PPt$	$C_{57}H_{38}F_6N_5PPt$	$C_{102}H_{69}F_6N_8O_4PPt_2$	$C_{132}H_{94}AgF_{16.5}N_{12}P_{2.75}Pt_2$
Crystal System	Orthorhombic	Monoclinic	Monoclinic	Monoclinic	Triclinic	Triclinic
a (Å)	15.3721(2)	20.8432(2)	22.0458(2)	16.9422(2)	17.4175(2)	17.4754(3)
b (Å)	17.0053(2)	29.6127(3)	9.63000(10)	17.69520(10)	17.4217(3)	24.8036(5)
c (Å)	30.0534(3)	17.6765(2)	23.7845(2)	18.3812(2)	17.9119(2)	28.7013(4)
α (°)	90	90	90	90	88.0990(10)	71.253(2)
β (°)	90	90.0950(10)	105.3730(10)	116.589(2)	65.5390(10)	76.9150(10)
γ (°)	90	90	90	90	67.428(2)	88.743(2)
V (Å^3)	7856.17(16)	10910.3(2)	4868.81(8)	4927.80(11)	4516.97(13)	11457.3(4)
Molecular weight	892.29	1155.76	1250.76	1132.98	2005.80	2744.90
Space group	$Pna2_1$	C2/c	$P2_1/c$	$P2_1/n$	P-1	P-1
μ (mm^{-1})	7.603	5.573	8.303	6.192	6.442	6.909
Temperature (K)	100(2)	100(2)	100(2)	100(2)	100(2)	100(2)
Z	8	8	4	8	2	4
D_{calc} (g/cm^3)	1.509	1.320	1.706	1.527	1.475	1.591
Crystal size (mm^3)	0.12 × 0.06 × 0.04	0.24 × 0.20 × 0.18	0.28 × 0.22 × 0.08	0.14 × 0.09× 0.05	0.1 × 0.06 × 0.04	0.05 × 0.02 × 0.01
Diffractometer	XtaLAB Synergy HyPix	SuperNova HyPix-3000	XtaLAB Synergy HyPix	XtaLAB Synergy HyPix	SuperNova HyPix-3000	SuperNova HyPix-3000
Radiation	Cu$K\alpha$	Cu$K\alpha$	Cu$K\alpha$	Cu$K\alpha$	Cu$K\alpha$	Cu$K\alpha$
Total reflections	60294	34174	57586	42306	53279	115952
Unique reflections	13358	10387	10258	10407	16700	42116
Angle range 2θ (°)	5.882 to 160.37	5.184 to 141.788	4.156 to 160.688	5.904 to 160.44	5.482 to 138.33	3.342 to 139.448
Reflections with $\lvert F_o \rvert \geq 4\sigma_F$	12199	9440	9556	9323	14807	32782
R_{int}	0.0402	0.0266	0.0476	0.0450	0.0354	0.0597
R_σ	0.0304	0.0239	0.0309	0.0379	0.0321	0.0547
R_1 ($\lvert F_o \rvert \geq 4\sigma_F$)	0.0428	0.0392	0.0311	0.0359	0.0542	0.0709
wR_2 ($\lvert F_o \rvert \geq 4\sigma_F$)	0.1119	0.1058	0.0756	0.0875	0.1461	0.1778
R_1 (all data)	0.0475	0.0422	0.0335	0.0398	0.0591	0.0929

wR_2 (all data)	0.1156	0.1086	0.0769	0.0898	0.1520	0.1962
S	1.057	1.042	1.082	1.088	1.044	1.057
ρ_{min}, ρ_{max}, e/Å^3	–1.67, 2.03	–0.93, 2.83	–0.94, 0.81	–1.10, 1.27	–1.53, 6.21	–1.79, 3.37
CCDC	2242753	2242764	2242765	2242766	2242769	2242797
$R_1 = \Sigma \lvert \lvert F_o \rvert - \lvert F_c \rvert \rvert / \Sigma \lvert F_o \rvert$; $wR_2 = \{\Sigma[w(F_o^2 - F_c^2)^2]/\Sigma[w(F_o^2)^2]\}^{1/2}$; $w = 1/[\sigma^2(F_o^2)+(aP)^2 + bP]$, where $P = (F_o^2 + 2F_c^2)/3$; $s = \{\Sigma[w(F_o^2 - F_c^2)]/(n - p)\}^{1/2}$ where n is the number of reflections and p is the number of refinement parameters.						

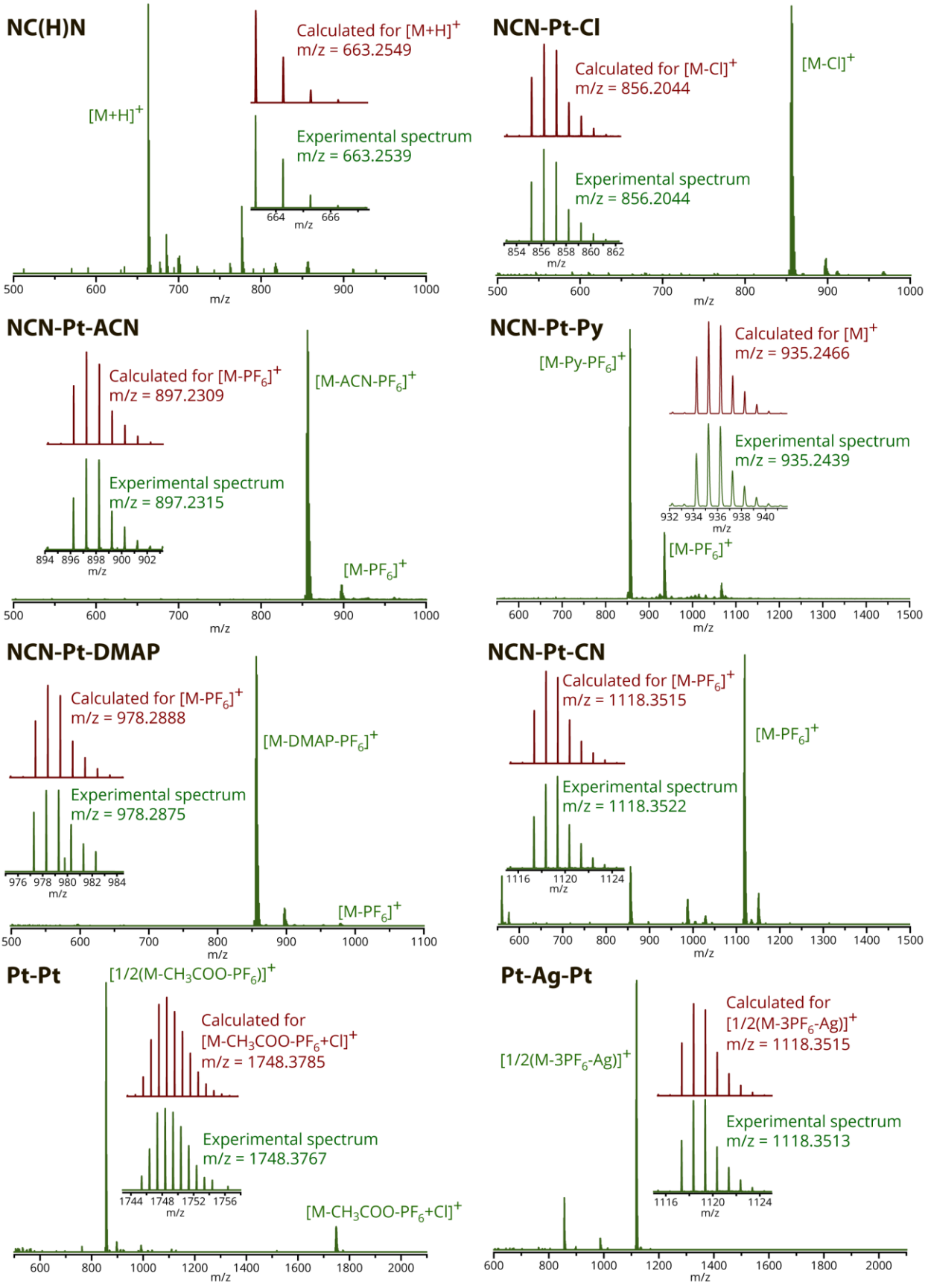

Figure S2. ESI⁺ mass-spectra of NC(H)N ligand and platinum complexes.

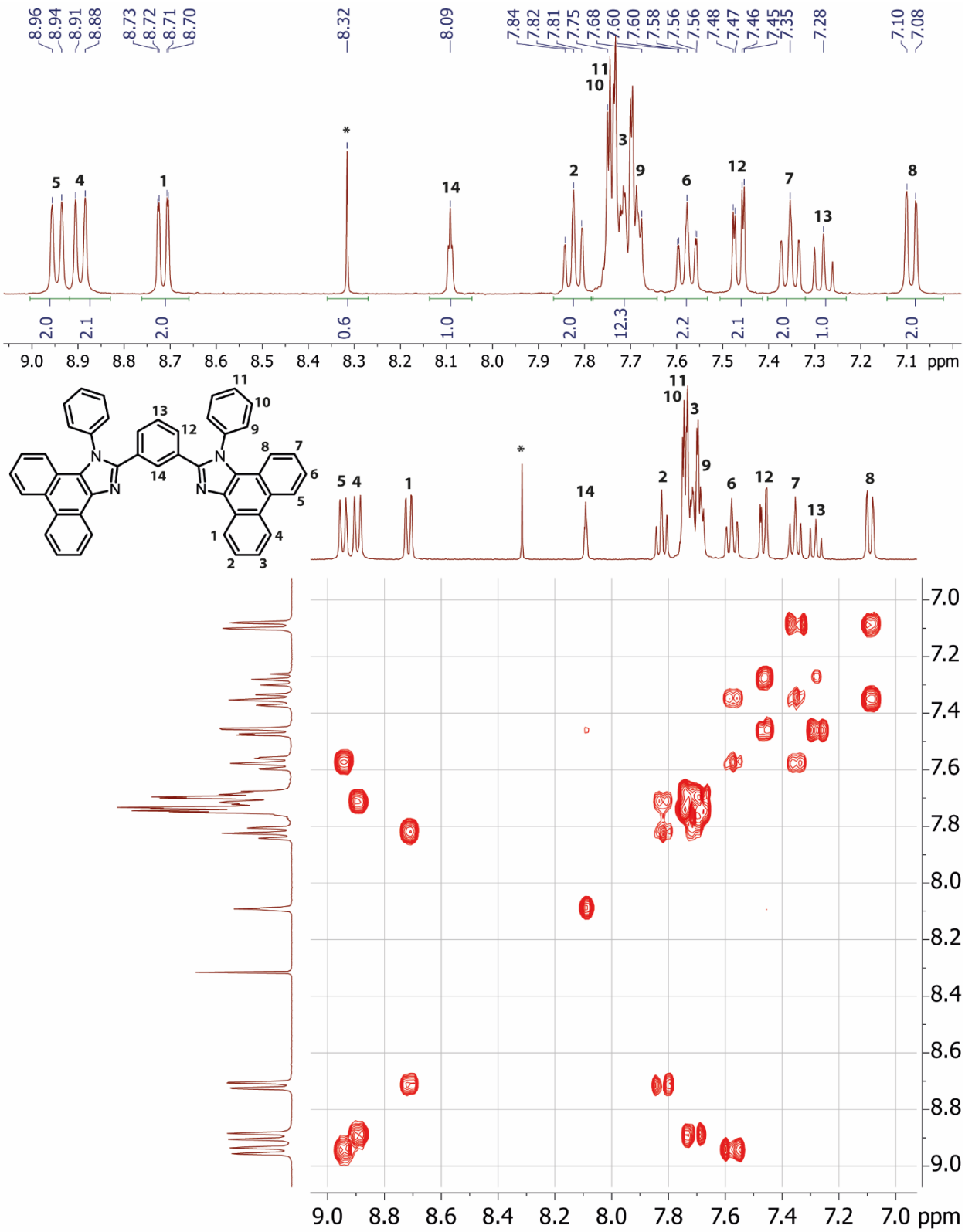

Figure S3. . ^{1}H and COSY NMR spectra of NC(H)N in DMSO-d6, 298 K.

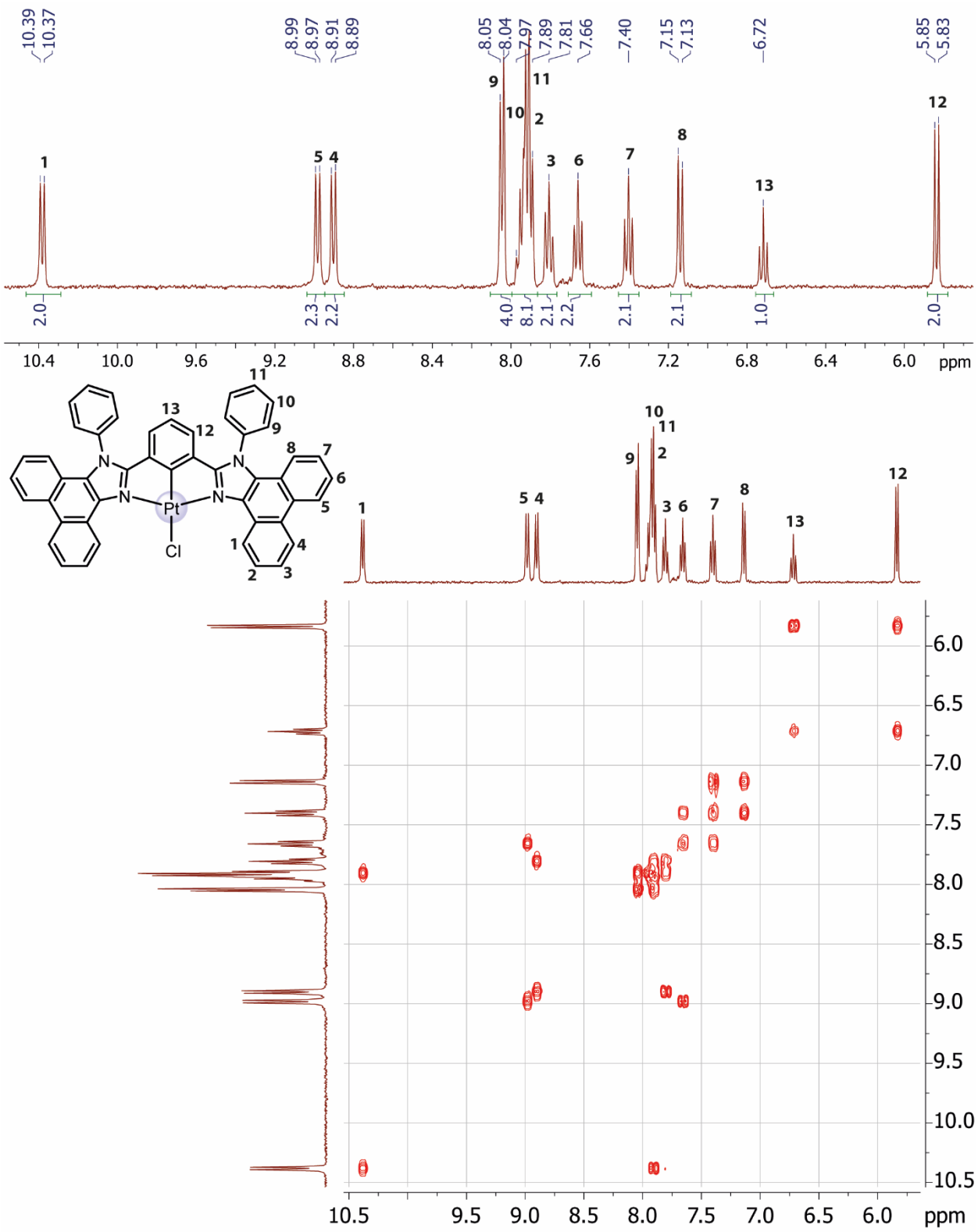

Figure S4. ^{1}H and COSY NMR spectra of NCN-Pt-Cl in DMSO-d6, 298 K.

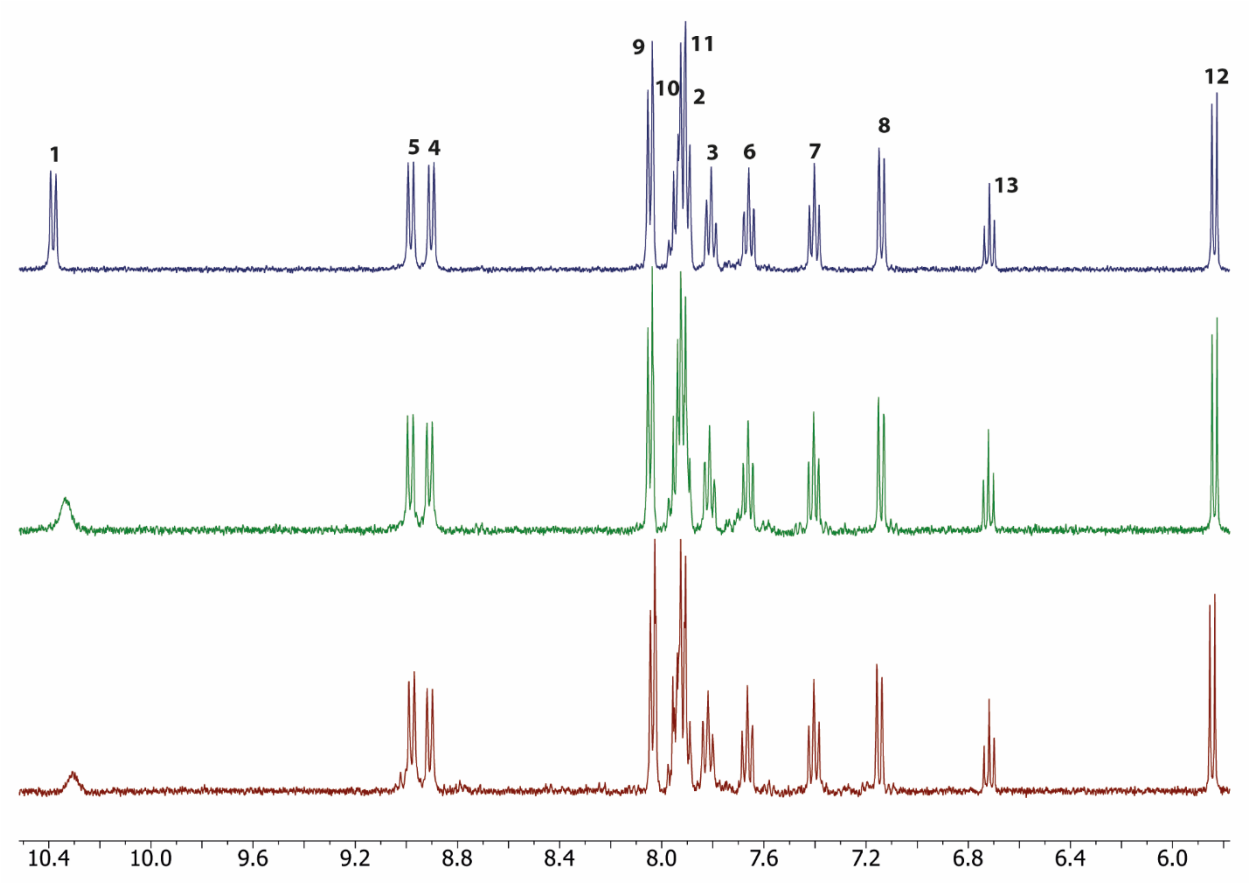

Figure S5. ^{1}H NMR spectra of NCN-Pt-Cl in DMSO-d6 at different concentrations, 298 K.

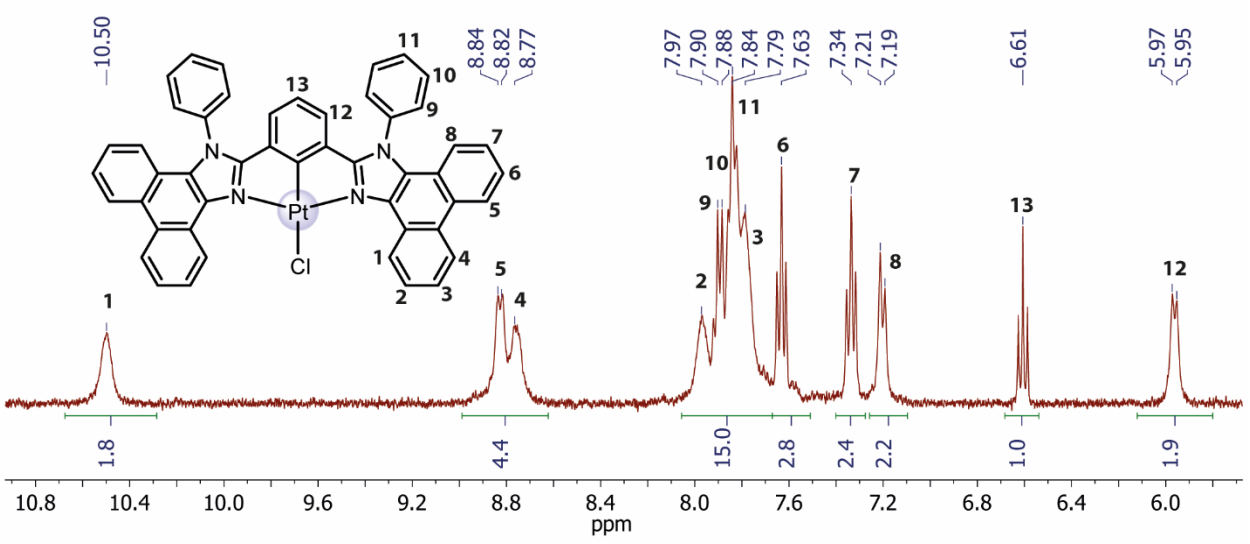

Figure S6. ^{1}H NMR spectrum of NCN-Pt-Cl in CD_2Cl_2, 298 K.

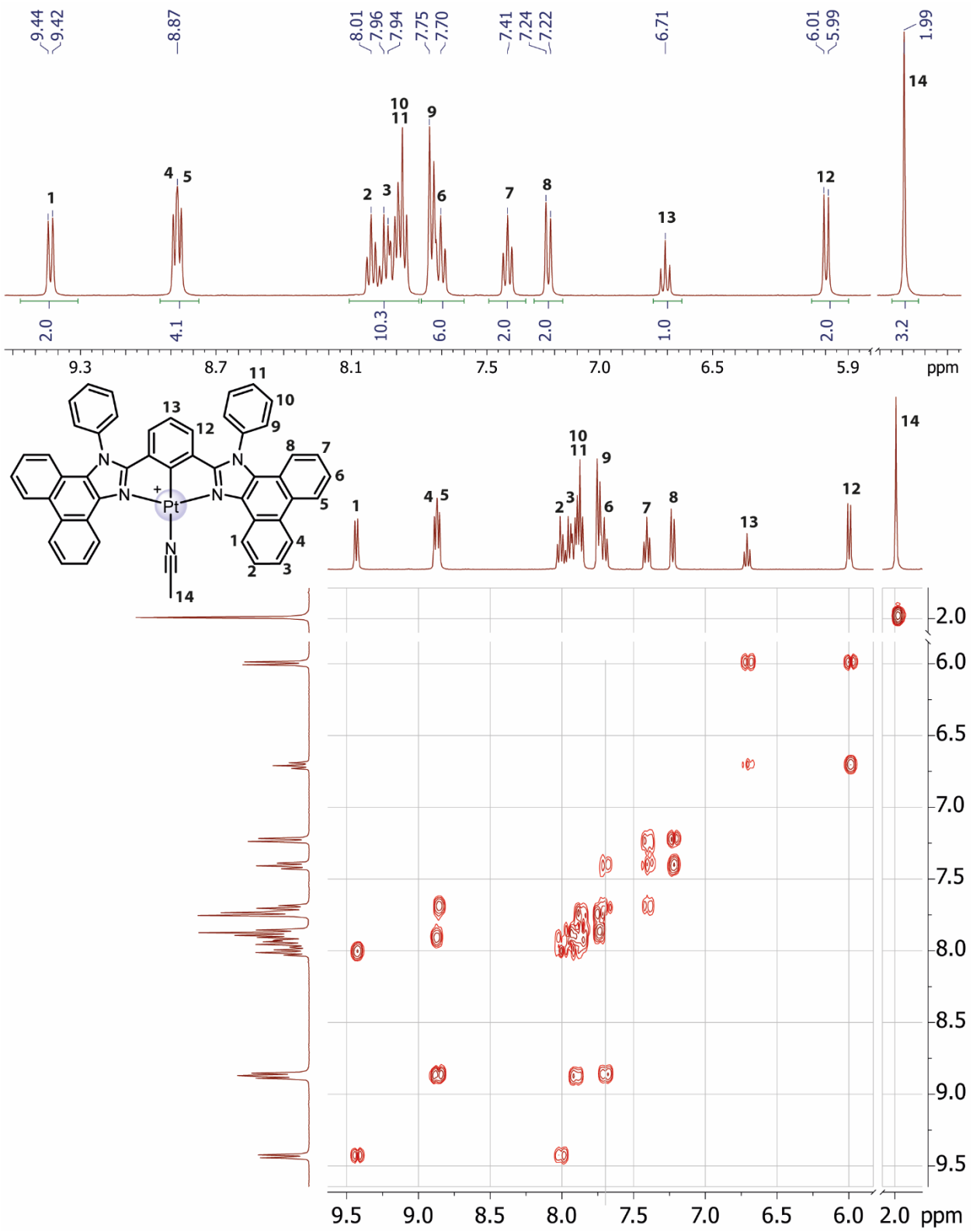

Figure S7. ^{1}H and COSY NMR spectra of NCN-Pt-ACN in CD_2Cl_2, 298 K.

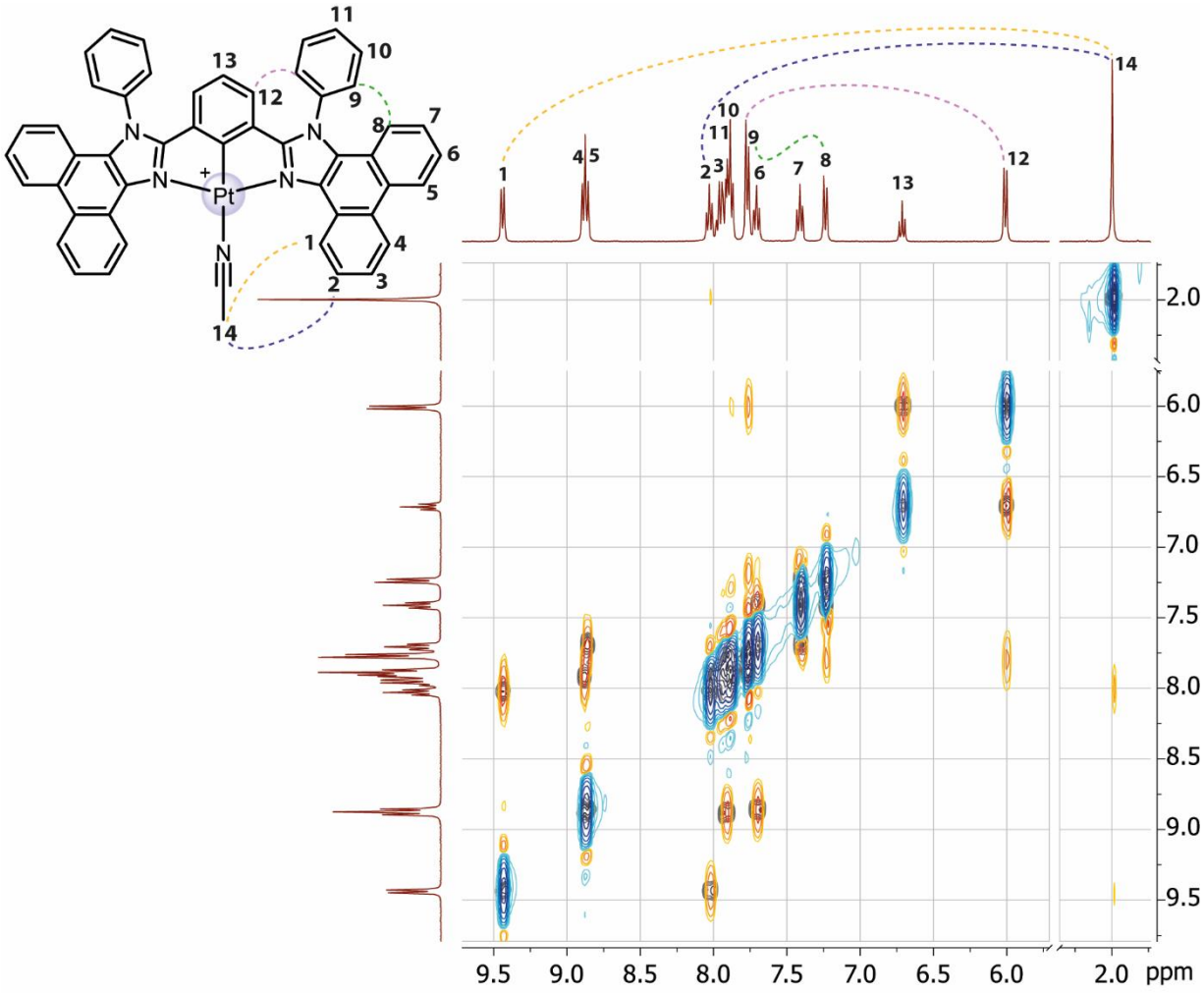

Figure S8. Overlapped ^{1}H-^{1}H COSY and NOESY NMR spectra of NCN-Pt-ACN with full assignment of the signals. Top-left structure of the complex shows atom numbering scheme, short contacts between protons revealed in the NOESY spectrum are also accompanied with the distances found in solid state structure.

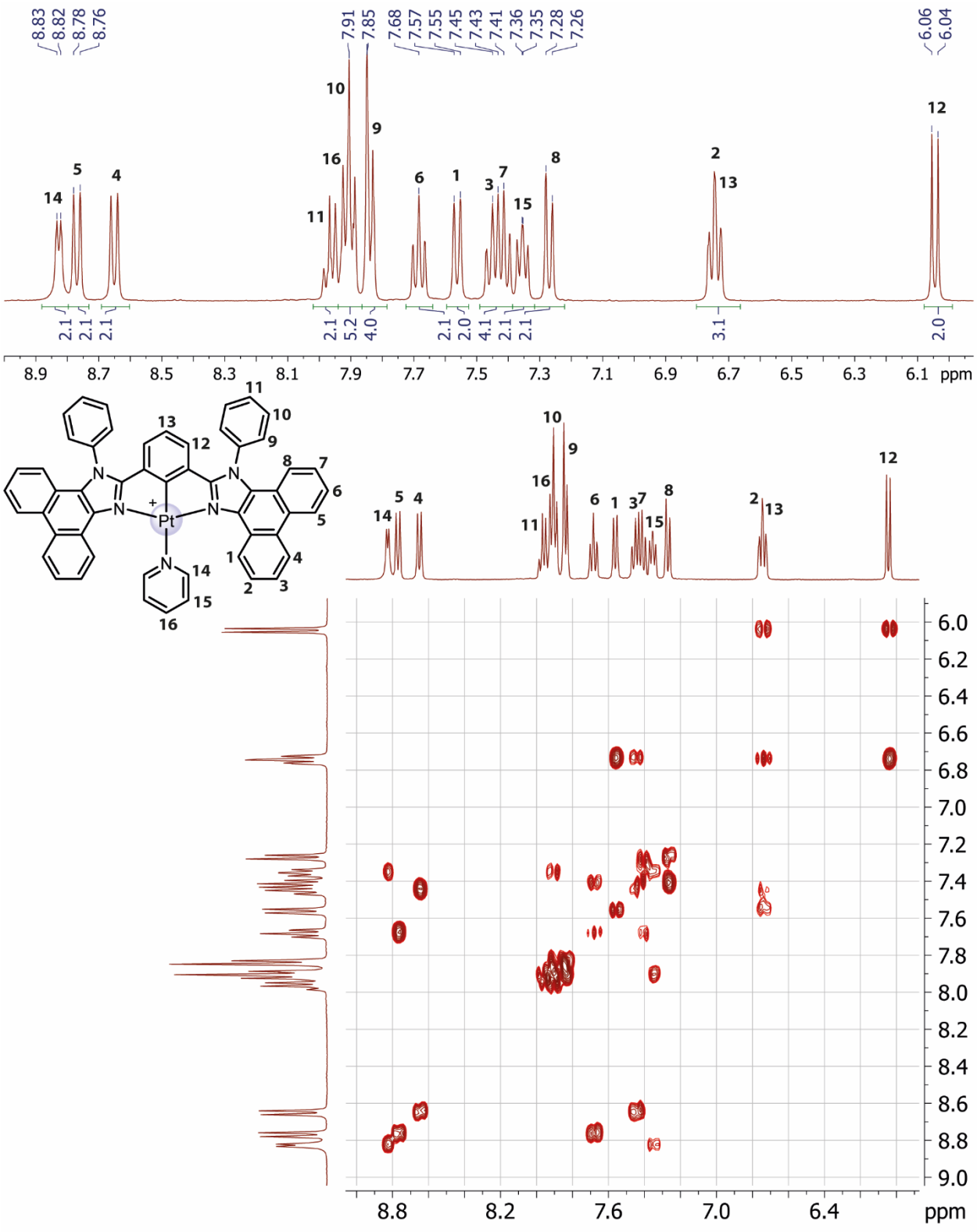

Figure S9. ^{1}H and COSY NMR spectra of NCN-Pt-Py in CD_2Cl_2, 298 K.

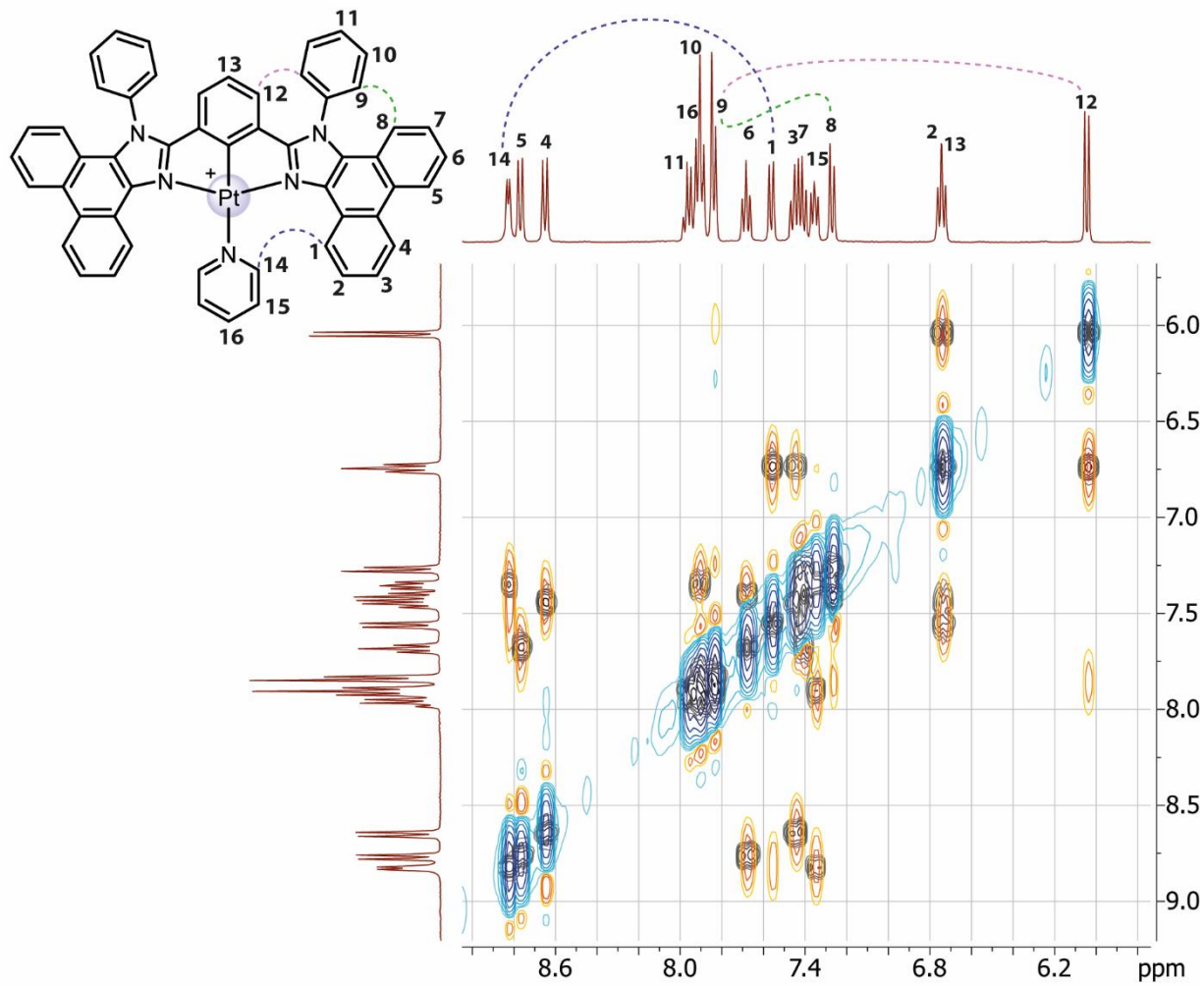

Figure S10. Overlapped ^{1}H-^{1}H COSY (gray) and NOESY (orange and blue) NMR spectra of NCN-Pt-Py with full assignment of the signals. Top-left structure of the complex shows atom numbering scheme.

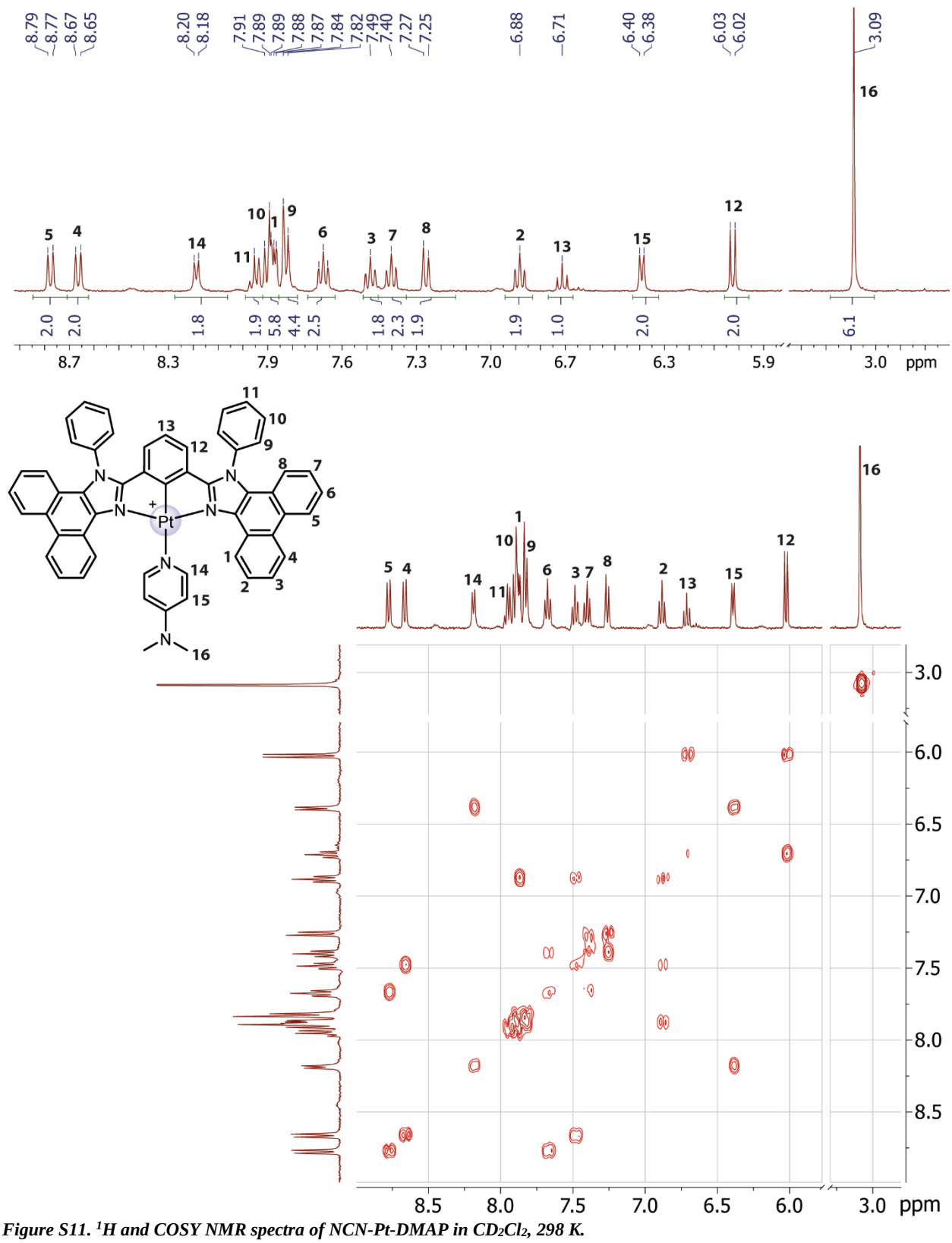

Figure S11. ^{1}H and COSY NMR spectra of NCN-Pt-DMAP in CD_2Cl_2, 298 K.

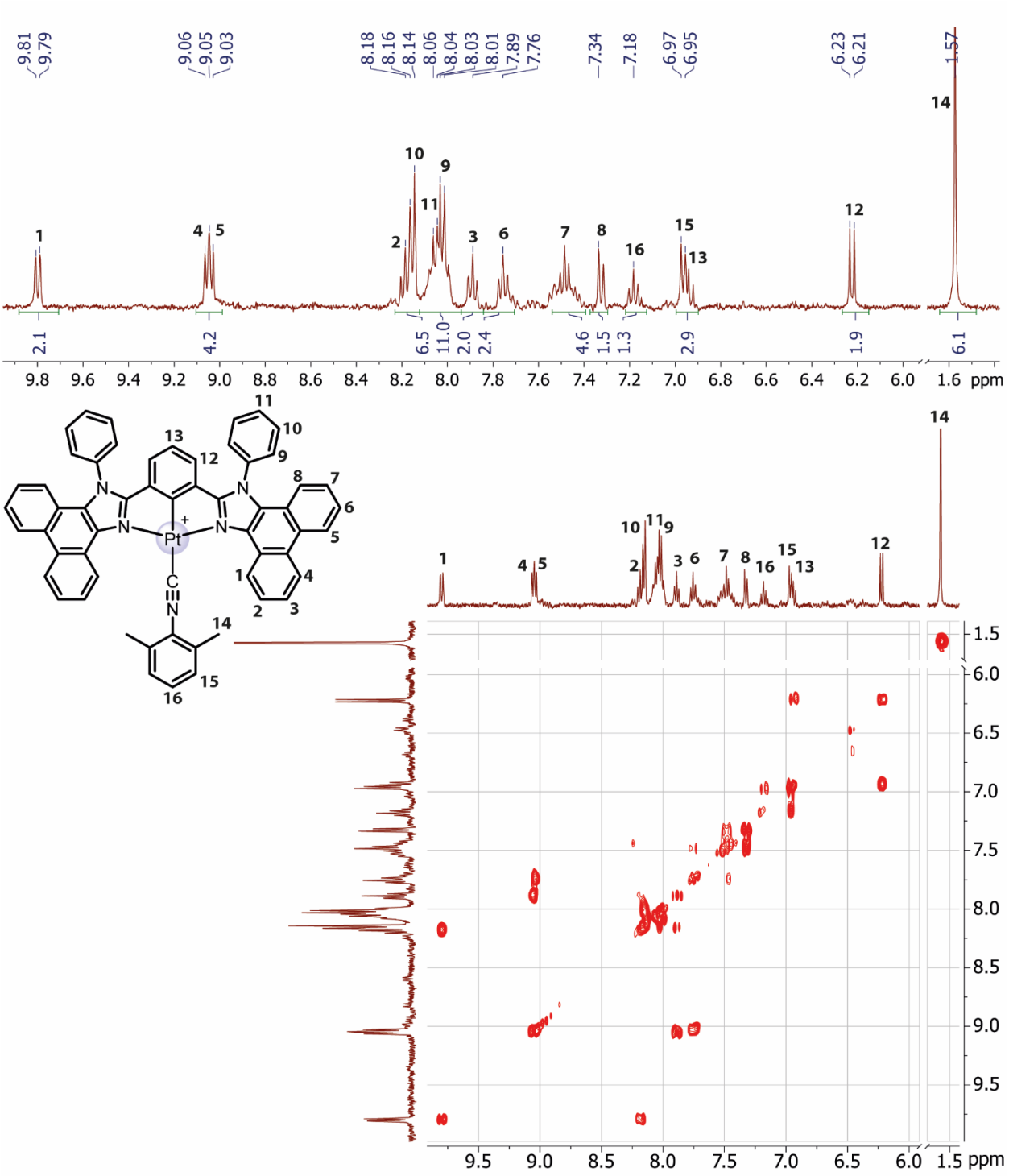

Figure S12. ^{1}H and COSY NMR spectra of NCN-Pt-CN in acetone-d6, 298 K.

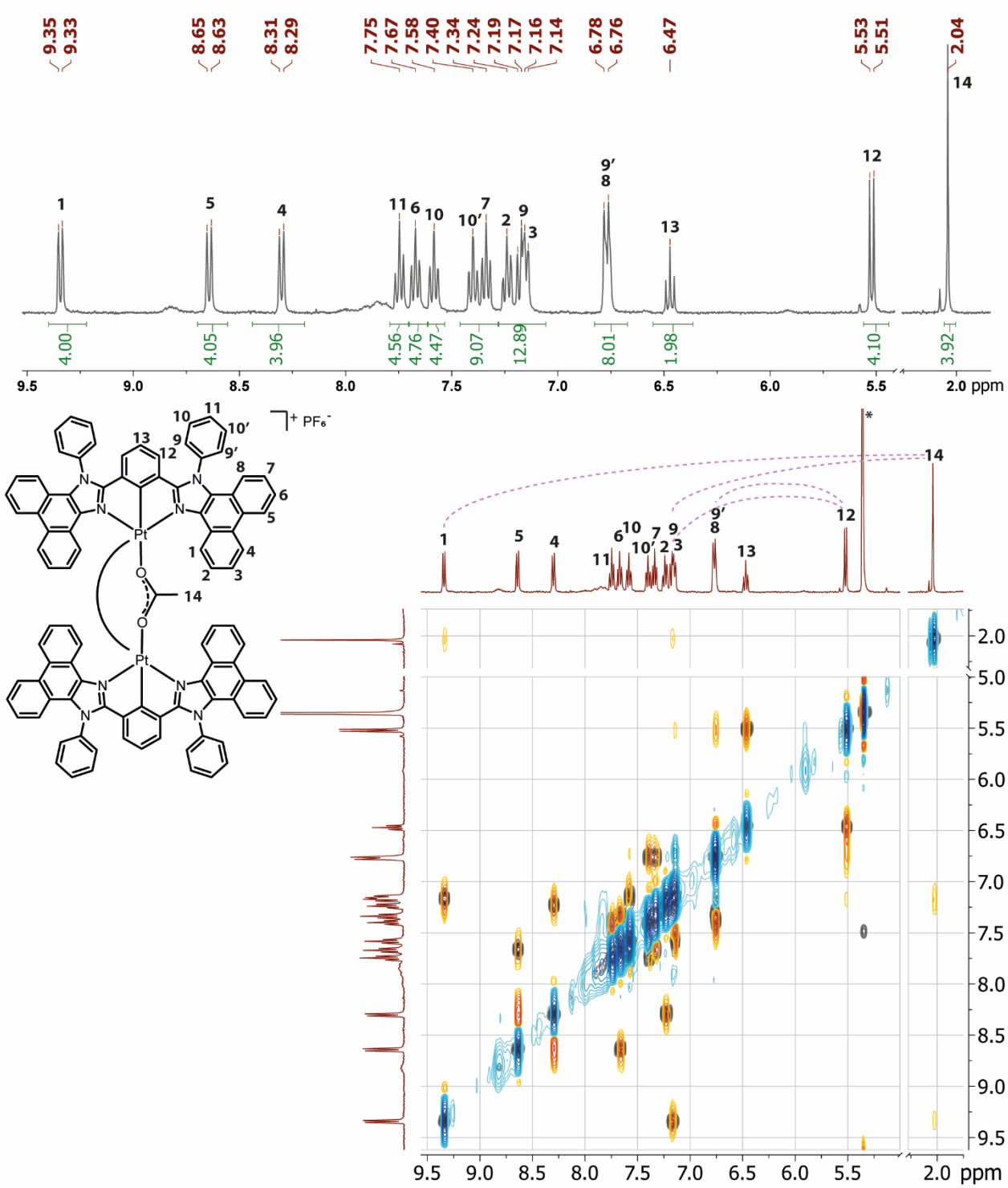

Figure S13. ^{1}H and overlapped ^{1}H-^{1}H COSY (gray) and NOESY (orange and blue) NMR spectra of Pt-Pt with full assignment of the signals, CD_2Cl_2, 298 K. Top-left structure of the complex shows atom numbering scheme.

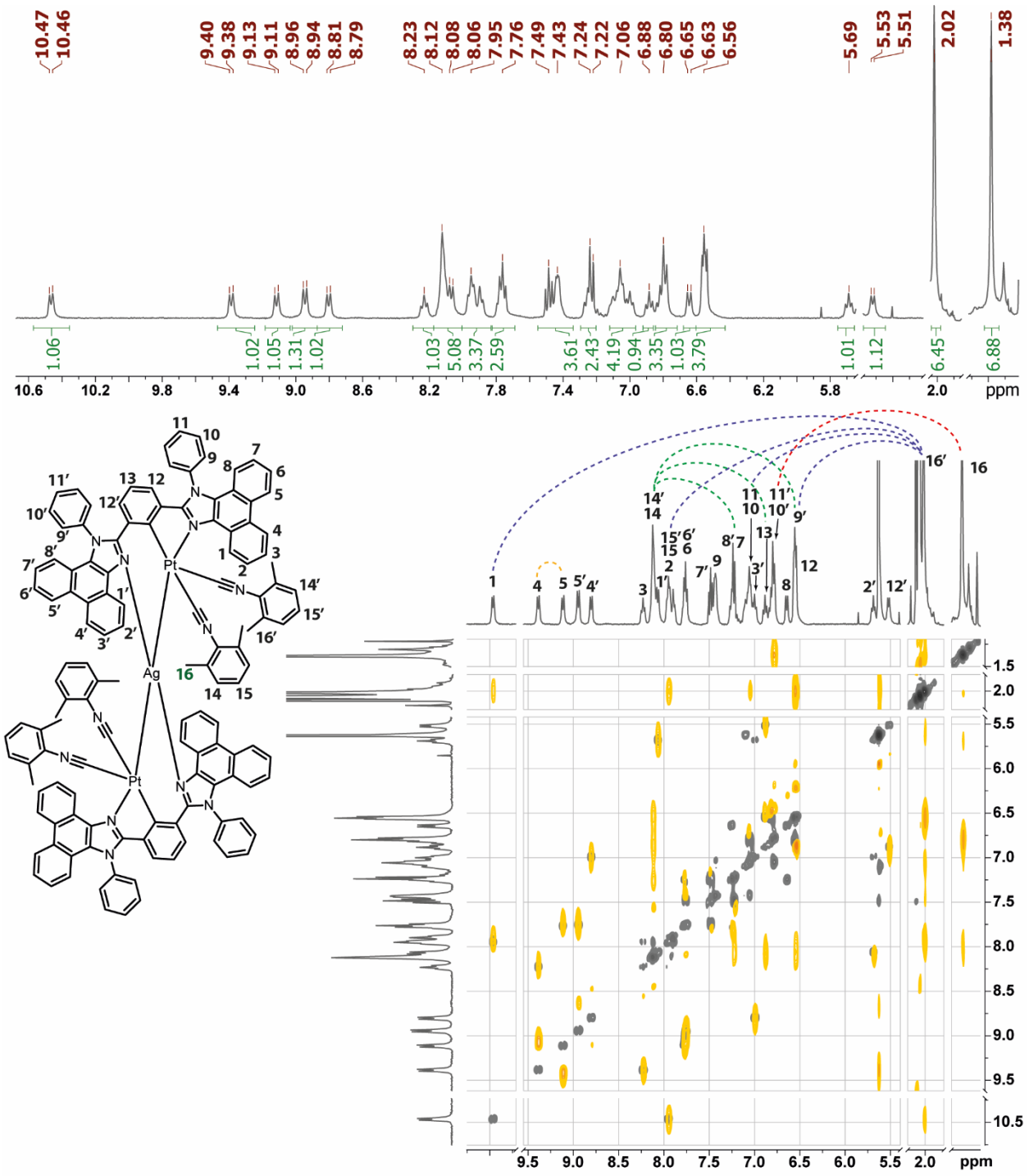

Figure S14. *^{1}H and overlapped ^{1}H-^{1}H COSY (gray) and NOESY (orange and blue) NMR spectra of Pt-Ag-Pt with full assignment of the signals, acetone-d6, 298 K. Top-left structure of the complex shows atom numbering scheme.*

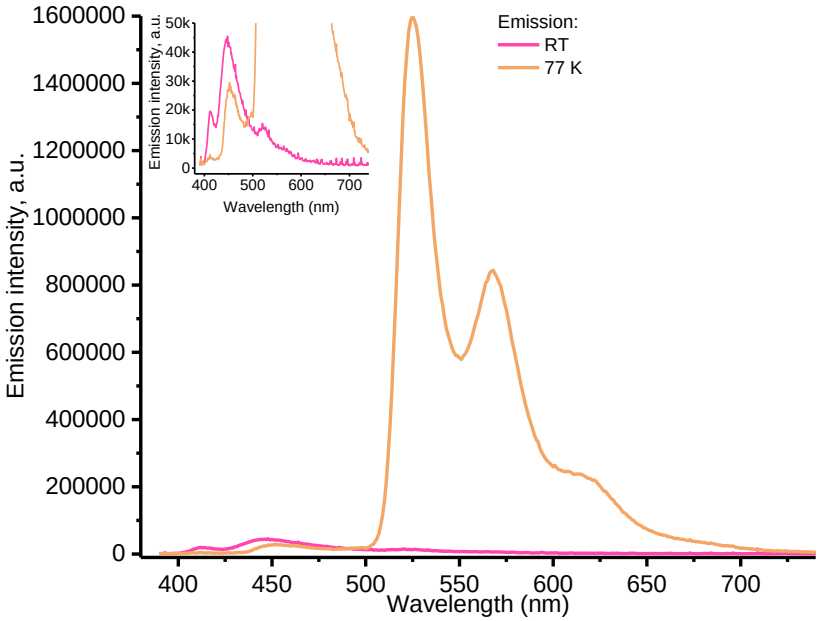

*Figure S15. Emission spectra NCN-Pt-Cl in DCM at RT and 77 K, c = 1*10^{-4} M.*

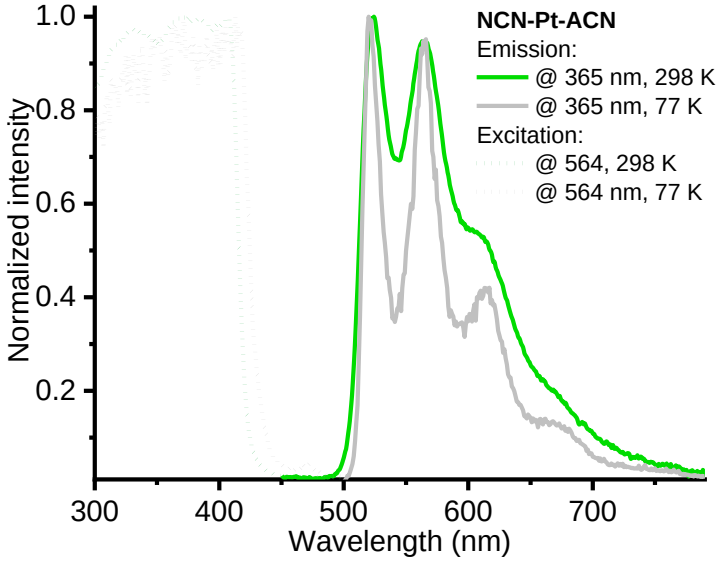

*Figure S16. Excitation (dashed line) and emission (solid line) spectra NCN-Pt-ACN in DCM at RT and 77 K, concentration = 1*10^{-4} M.*

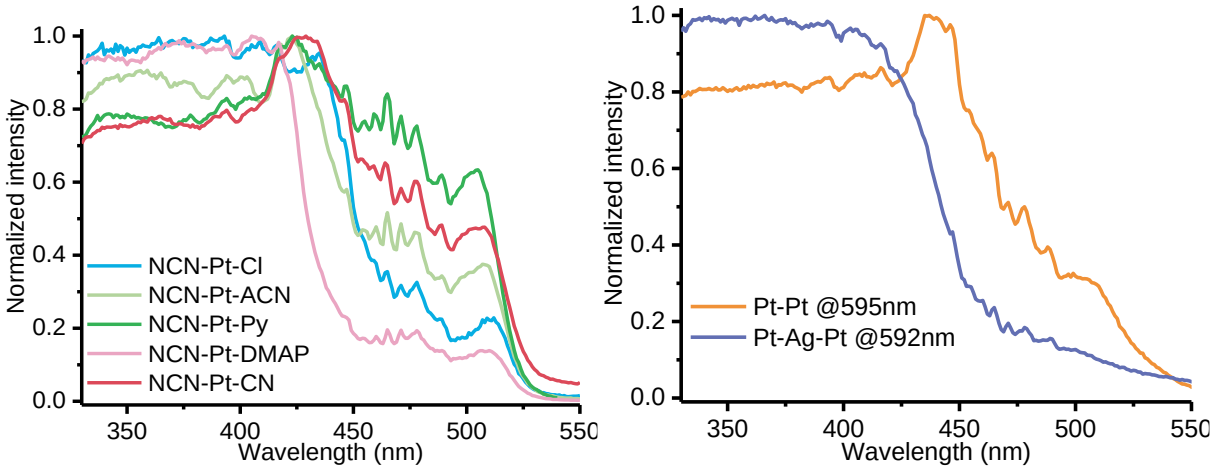

Figure S17. Excitation spectra of complexes in the solid state, λ_{em} = 566 nm for mononuclear complexes, 298 K.

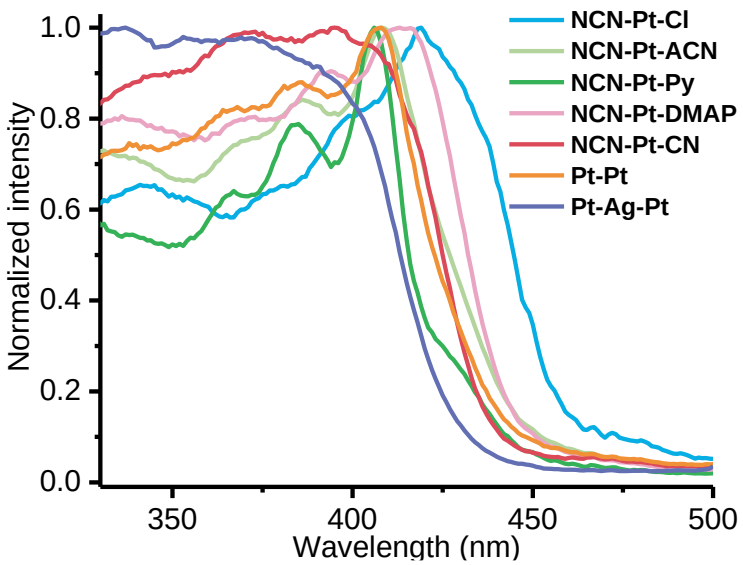

Figure S18. Excitation spectra of complexes in PMMA film, λ_{em} – emission maximum, 298 K.

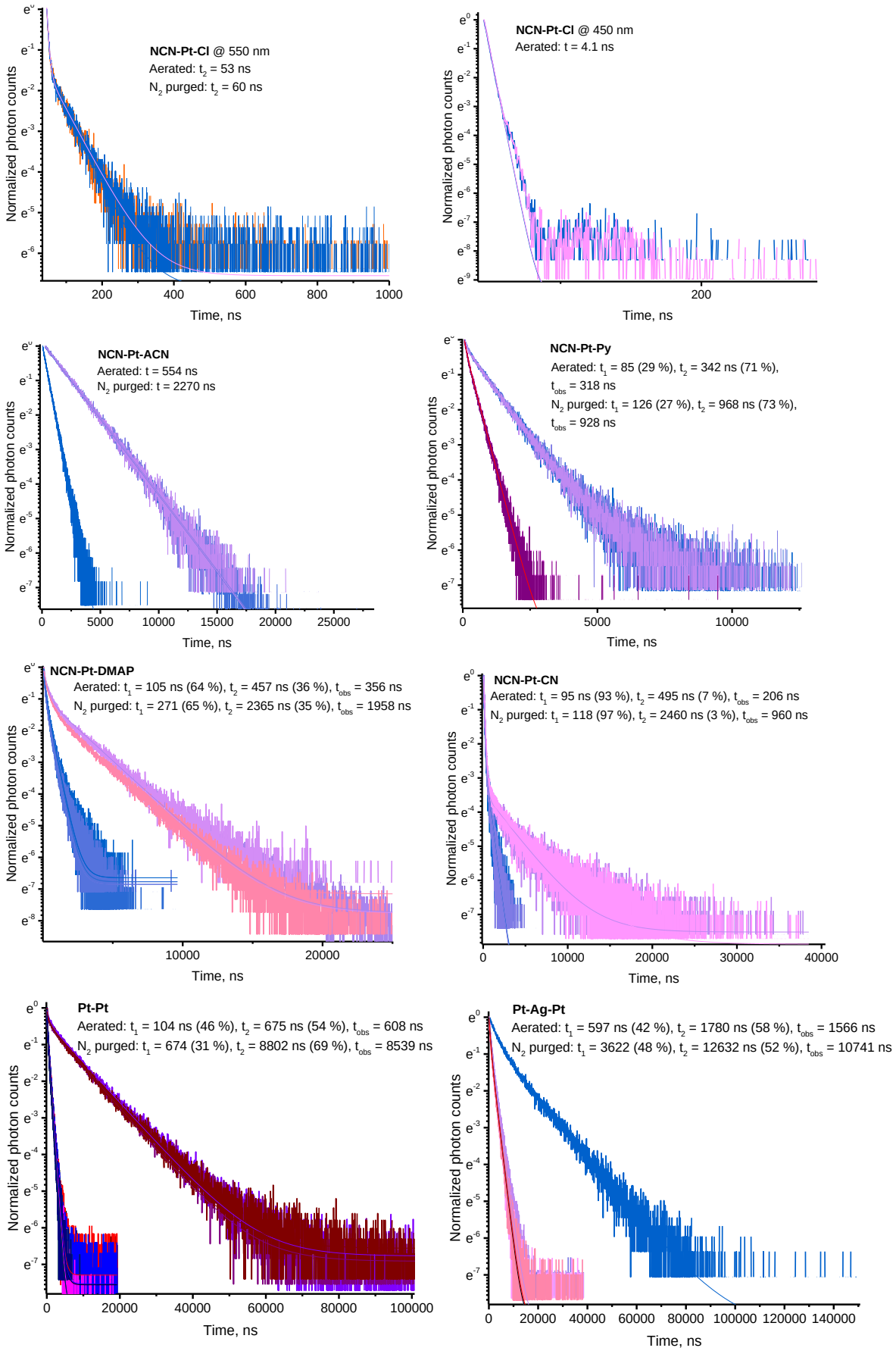

Figure S19. Lifetime decays of complexes in aerated and argon purged DCM solutions, λ_{ex} = 355 nm.

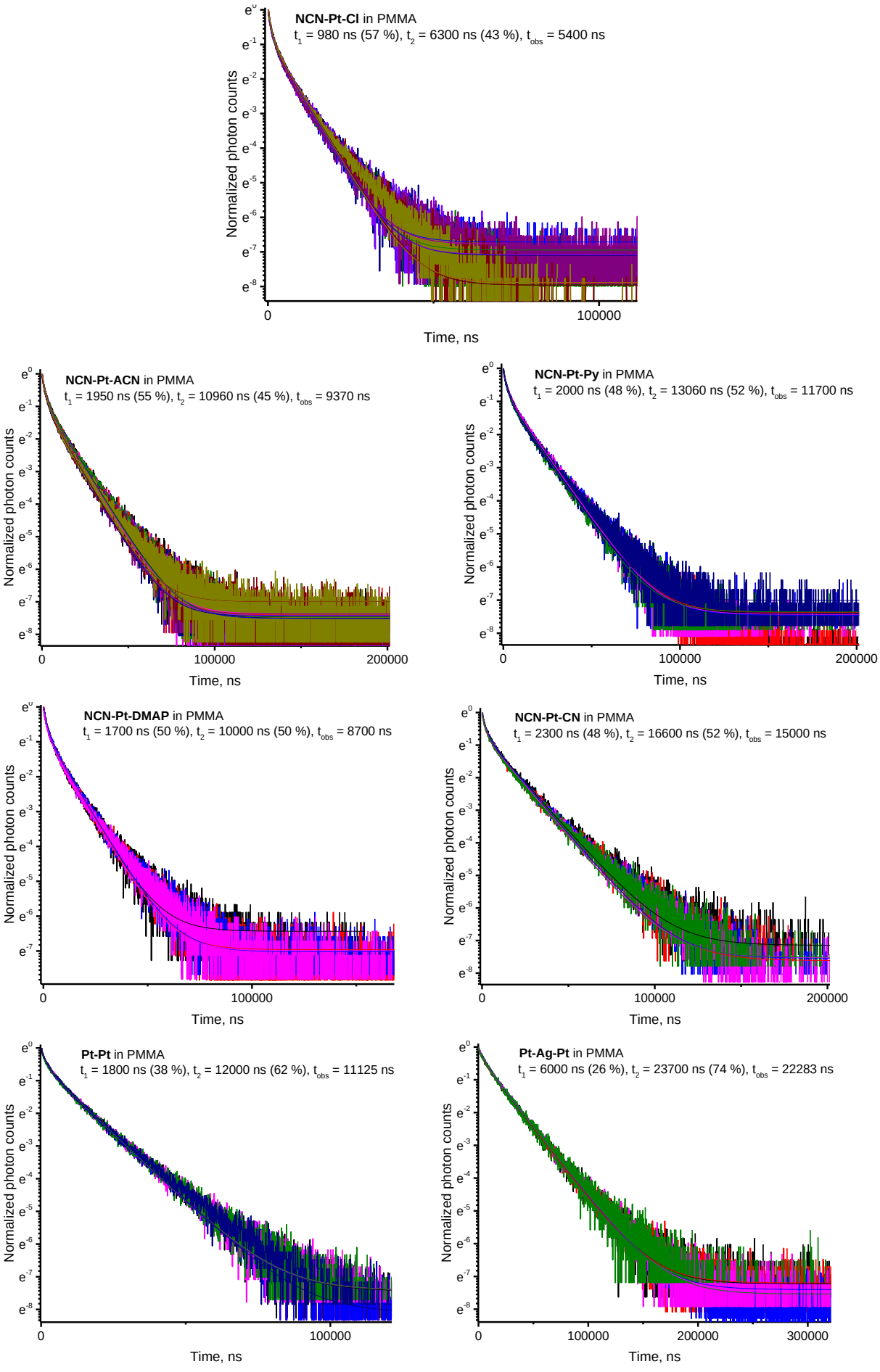

Figure S20. Lifetime decays of complexes in PMMA, λ_{ex} = 355 nm.

Table S3. Calculated absorption maxima (λ) and oscillator strengths (f) of NCN-Pt-Cl.

Transitions	λ, nm (calc)	*f* (calc)	Contribution of main NTO pair in transition (%)
$S_0 \rightarrow S_4$	251	0.19	32
$S_0 \rightarrow S_3$	298	0.20	46
$S_0 \rightarrow S_2$	349	0.13	52
$S_0 \rightarrow S_1$	393	0.58	97

Table S4. The decrease (violet) and increase (terracota) of electron density for most intensive electronic absorption transitions of NCN-Pt-Cl. The data for the corresponding interfragment charge transfer (IFCT) are given below the figures. Diagonal values represent intraligand transitions, off-diagonal values represent a charge transfer from "Donor" to "Acceptor".

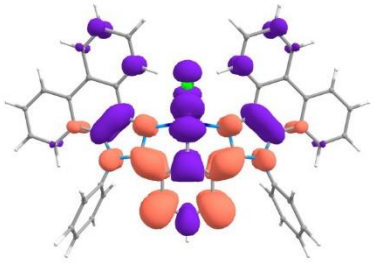

S_0-S_1

	Acceptor		
Donor	Pt	Cl	NCN
Pt	0.001	0.000	0.167
Cl	0.001	0.000	0.075
NCN	0.006	0.000	0.751

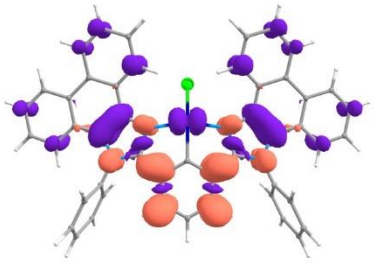

S_0-S_2

	Acceptor		
Donor	Pt	Cl	NCN
Pt	0.016	0.001	0.143
Cl	0.006	0.000	0.055
NCN	0.080	0.002	0.696

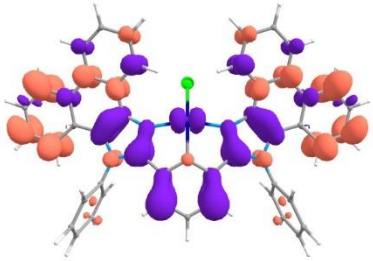

S_0-S_3

	Acceptor		
Donor	Pt	Cl	NCN
Pt	0.001	0.000	0.073
Cl	0.000	0.000	0.025
NCN	0.015	0.000	0.886

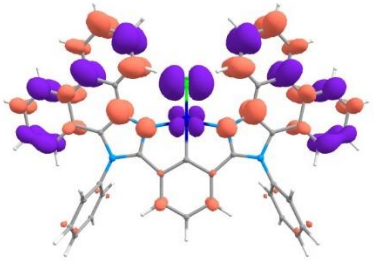

S_0-S_4

	Acceptor		
Donor	Pt	Cl	NCN
Pt	0.051	0.000	0.053
Cl	0.038	0.000	0.040
NCN	0.398	0.001	0.418

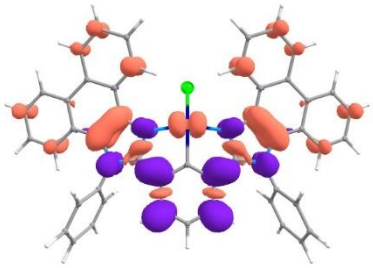

T_1-S_0

	Acceptor		
Donor	Pt	Cl	NCN
Pt	0.003	0.000	0.034
Cl	0.000	0.000	0.001

NCN	0.077	0.009	0.876

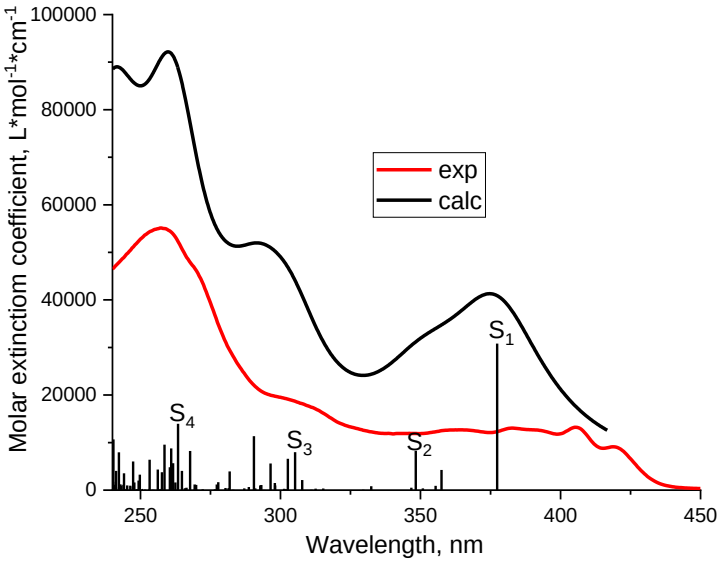

Figure S21. Absorption spectra of NCN-Pt-Py: experimental (red) and calculated (black) lines with oscillator strengths of electronic transitions (bars).

Table S5. Calculated absorption maxima (λ) and oscillator strengths (f) of NCN-Pt-Py.

Transitions	λ, nm (calc)	*f* (calc)	Contribution of main NTO pair in transition (%)
$S_0 \rightarrow S_4$	263	0.28	46
$S_0 \rightarrow S_3$	305	0.16	77
$S_0 \rightarrow S_2$	348	0.17	68
$S_0 \rightarrow S_1$	377	0.63	97

Table S6. The decrease (violet) and increase (terracota) of electron density for most intensive electronic absorption transitions of NCN-Pt-Py. The data for the corresponding interfragment charge transfer (IFCT) are given below the figures. Diagonal values represent intraligand transitions, off-diagonal values represent a charge transfer from "Donor" to "Acceptor".

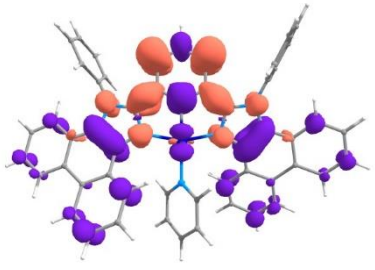

S_0-S_1

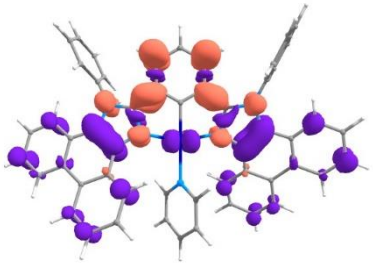

S_0-S_2

	Acceptor				Acceptor		
Donor	Pt	Py	NCN	Donor	Pt	Py	NCN
Pt	0.001	0.000	0.061	Pt	0.008	0.006	0.046
Py	0.000	0.000	0.007	Py	0.000	0.000	0.002
NCN	0.011	0.000	0.922	NCN	0.125	0.097	0.717

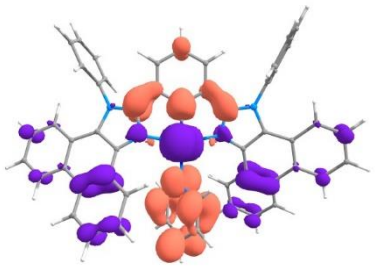

S_0-S_3

	Acceptor		
Donor	Pt	Py	NCN
Pt	0.053	0.111	0.228
Py	0.001	0.002	0.004
NCN	0.081	0.170	0.349

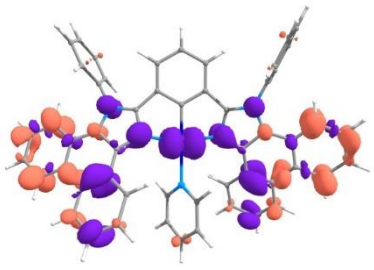

S_0-S_4

	Acceptor		
Donor	Pt	Py	NCN
Pt	0.014	0.002	0.114
Py	0.000	0.000	0.002
NCN	0.096	0.014	0.758

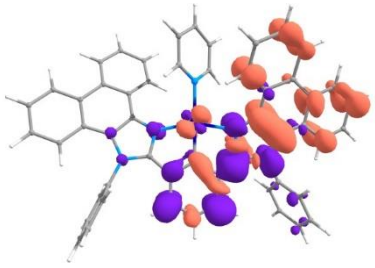

T_1-S_0

	Acceptor		
Donor	Pt	Py	NCN
Pt	0.000	0.000	0.000
Py	0.000	0.008	0.070
NCN	0.000	0.114	1.023

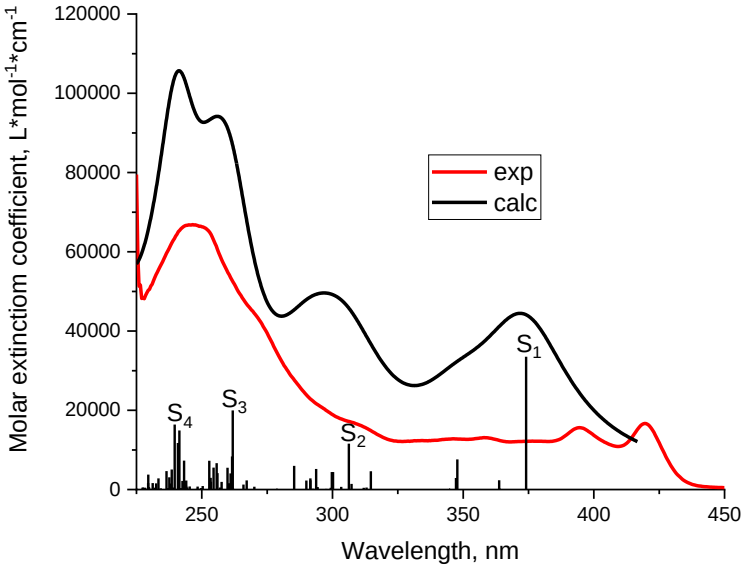

Figure S22. Absorption spectra of NCN-Pt-ACN: experimental (red) and calculated (black) lines with oscillator strengths of electronic transitions (bars).

Table S7. Calculated absorption maxima (λ) and oscillator strengths (f) of NCN-Pt-ACN.

Transitions	λ, nm (calc)	*f* (calc)	Contribution of main NTO pair in transition (%)
$S_0 \rightarrow S_4$	240	0.33	43
$S_0 \rightarrow S_3$	262	0.41	74
$S_0 \rightarrow S_2$	306	0.24	46
$S_0 \rightarrow S_1$	374	0.68	93

Table S8. The decrease (violet) and increase (terracota) of electron density for most intensive electronic absorption transitions of NCN-Pt-ACN. The data for the corresponding interfragment charge transfer (IFCT) are given below the figures. Diagonal values represent intraligand transitions, off-diagonal values represent a charge transfer from "Donor" to "Acceptor".

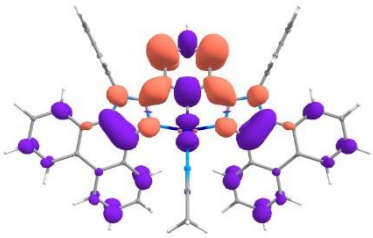

S_0-S_1

	Acceptor		
Donor	Pt	ACN	NCN
Pt	0.001	0.000	0.064
ACN	0.000	0.000	0.007
NCN	0.018	0.003	0.907

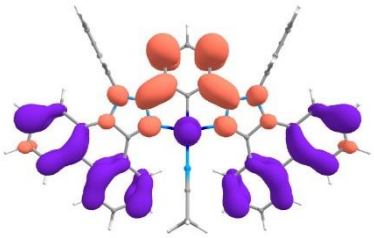

S_0-S_2

	Acceptor		
Donor	Pt	ACN	NCN
Pt	0.010	0.001	0.087
ACN	0.000	0.000	0.003
NCN	0.095	0.009	0.796

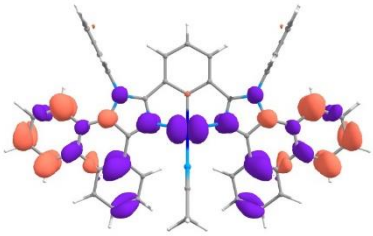

S_0-S_3

	Acceptor		
Donor	Pt	ACN	NCN
Pt	0.008	0.000	0.127
ACN	0.000	0.000	0.002
NCN	0.053	0.000	0.809

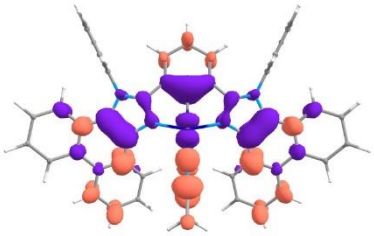

S_0-S_4

	Acceptor		
Donor	Pt	ACN	NCN
Pt	0.007	0.009	0.119
ACN	0.000	0.000	0.007
NCN	0.044	0.056	0.758

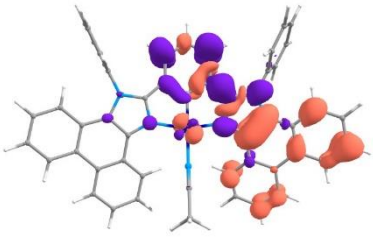

T_1-S_0

	Acceptor		
Donor	Pt	ACN	NCN
Pt	0.002	0.000	0.043
ACN	0.001	0.000	0.011
NCN	0.049	0.003	0.892

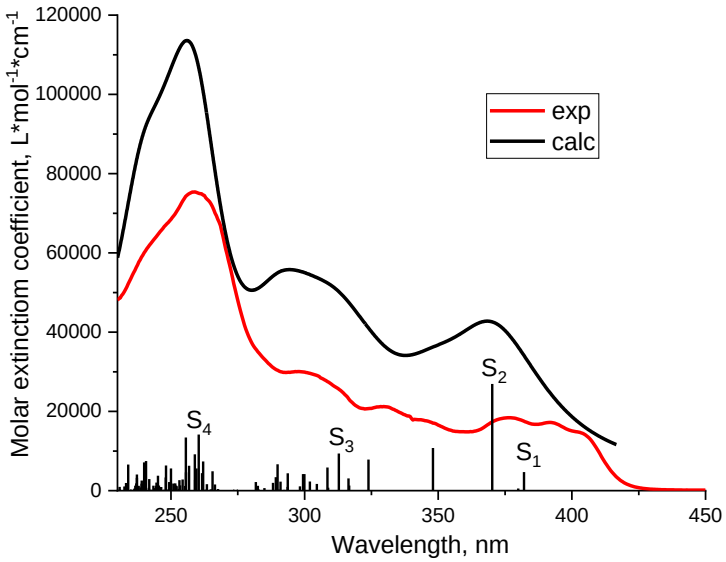

Figure S23. Absorption spectra of NCN-Pt-CN: experimental (red) and calculated (black) lines with oscillator strengths of electronic transitions (bars).

Table S9. Calculated absorption maxima (λ) and oscillator strengths (f) of NCN-Pt-CN.

Transitions	λ, nm (calc)	*f* (calc)	Contribution of main NTO pair in transition (%)
$S_0 \rightarrow S_4$	260	0.29	42
$S_0 \rightarrow S_3$	313	0.19	76
$S_0 \rightarrow S_2$	370	0.55	96
$S_0 \rightarrow S_1$	382	0.10	96

Table S10. The decrease (violet) and increase (terracota) of electron density for most intensive electronic absorption transitions of NCN-Pt-CN. The data for the corresponding interfragment charge transfer (IFCT) are given below the figures. Diagonal values represent intraligand transitions, off-diagonal values represent a charge transfer from "Donor" to "Acceptor".

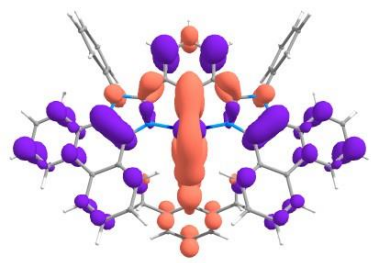

S_0-S_1

	Acceptor		
Donor	Pt	CN	NCN
Pt	0.006	0.009	0.017
CN	0.000	0.000	0.000
NCN	0.187	0.261	0.519

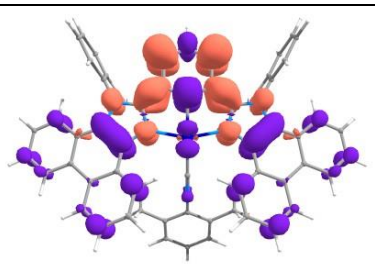

S_0-S_2

	Acceptor		
Donor	Pt	CN	NCN
Pt	0.000	0.000	0.043
CN	0.000	0.000	0.025
NCN	0.006	0.000	0.924

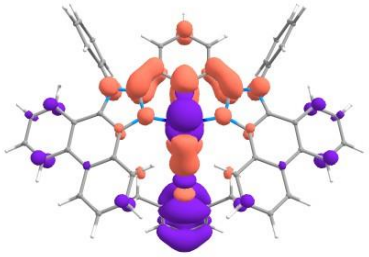

S_0-S_3

	Acceptor		
Donor	Pt	CN	NCN
Pt	0.043	0.053	0.133
CN	0.072	0.088	0.221
NCN	0.074	0.090	0.227

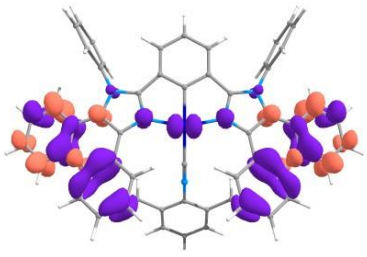

S_0-S_4

	Acceptor		
Donor	Pt	CN	NCN
Pt	0.002	0.001	0.099
CN	0.002	0.001	0.070
NCN	0.018	0.007	0.800

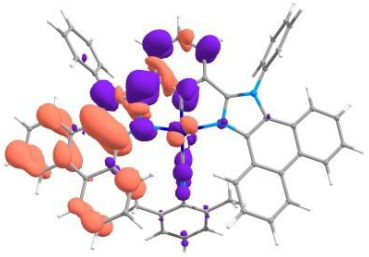

T_1-S_0

	Acceptor		
Donor	Pt	CN	NCN
Pt	0.003	0.001	0.067
CN	0.003	0.001	0.079
NCN	0.031	0.008	0.807

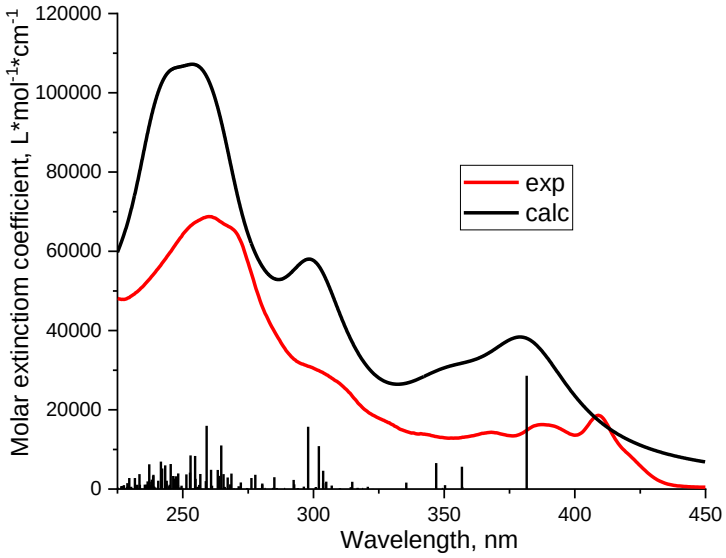

Figure S24. Absorption spectra of NCN-Pt-DMAP: experimental (red) and calculated (black) lines with oscillator strengths of electronic transitions (bars).

Table S11. Calculated absorption maxima (λ) and oscillator strengths (f) of NCN-Pt-DMAP.

Transitions	λ, nm (calc)	*f* (calc)	Contribution of main NTO pair in transition (%)
$S_0 \rightarrow S_4$	259	0.32	43
$S_0 \rightarrow S_3$	298	0.32	58
$S_0 \rightarrow S_2$	347	0.13	53
$S_0 \rightarrow S_1$	382	0.58	97

Table S12. The decrease (violet) and increase (terracota) of electron density for most intensive electronic absorption transitions of NCN-Pt-DMAP. The data for the corresponding interfragment charge transfer (IFCT) are given below the figures. Diagonal values represent intraligand transitions, off-diagonal values represent a charge transfer from "Donor" to "Acceptor".

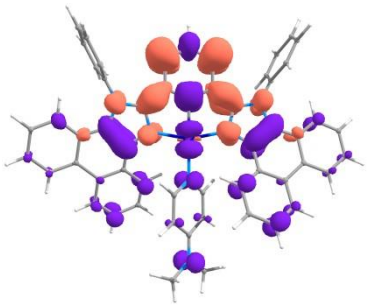

S_0-S_1

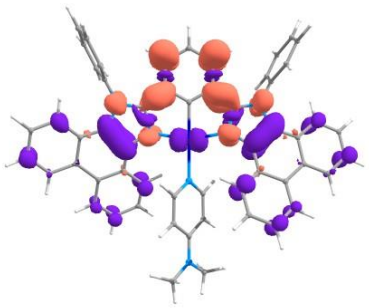

S_0-S_2

	Acceptor		
Donor	Pt	DMAP	NCN
Pt	0.001	0.000	0.085
DMAP	0.001	0.000	0.084
NCN	0.010	0.000	0.820

	Acceptor		
Donor	Pt	DMAP	NCN
Pt	0.011	0.000	0.064
DMAP	0.006	0.000	0.033
NCN	0.128	0.003	0.755

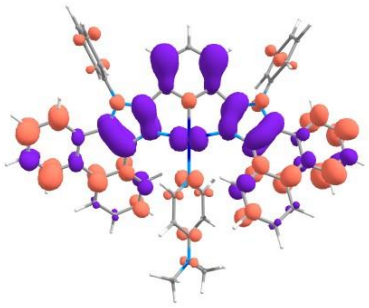

S_0-S_3

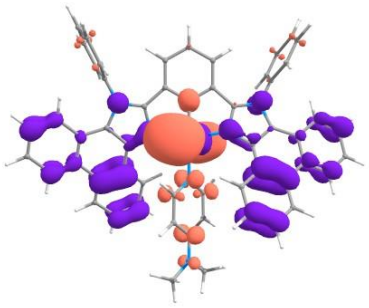

S_0-S_4

	Acceptor		
Donor	Pt	DMAP	NCN
Pt	0.006	0.003	0.050
DMAP	0.002	0.001	0.014
NCN	0.096	0.043	0.786

	Acceptor		
Donor	Pt	DMAP	NCN
Pt	0.056	0.009	0.068
DMAP	0.024	0.004	0.029
NCN	0.338	0.059	0.411

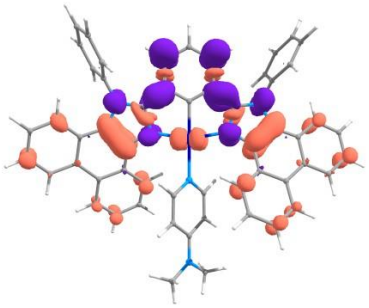

T_1-S_0			
	Acceptor		
Donor	Pt	DMAP	NCN
Pt	0.003	0.000	0.042
DMAP	0.000	0.000	0.002
NCN	0.057	0.007	0.889